

# Effect of Waves on Cavitation and Pressure Pulses of a Tanker with Twin Podded Propulsion

Bhushan Taskar<sup>a</sup>, Sverre Steen<sup>a</sup>, Jonas Eriksson<sup>b</sup>

<sup>a</sup> Department of Marine Technology, Norwegian University of Science and Technology (NTNU), Trondheim, Norway

<sup>b</sup> Rolls-Royce Marine AS, Norway

Corresponding Author: Bhushan Taskar ([bhushan.taskar@ntnu.no](mailto:bhushan.taskar@ntnu.no), Tel: +47 47167689)

## Abstract

There is increasing interest in optimizing ships for the actual operating condition rather than just for calm water. In order to optimize the propeller designs for operations in waves, it is essential to study how the propeller performance is affected by operation in waves. The effect of various factors that influence the propeller is quantified in this paper using a 8000 dwt chemical tanker equipped with twin-podded propulsion as a case vessel. Propeller performance in waves in terms of cavitation, pressure pulses, and efficiency is compared with the performance in calm water. The influence of wake variation, ship motions, RPM fluctuations and speed loss is studied. Substantial increase in cavitation and pressure pulses due to wake variation in the presence of waves is found. It is found that the effect of other factors is relatively small and easier to take into account as compared to wake variation. Therefore, considering the wake variation at least in the critical wave condition (where the wavelength is close to ship length) in addition to calm water wake is recommended in order to ensure that the optimized propeller performs well both in calm water and in waves.

**Keywords:** Propulsion in Waves, Cavitation, Pressure Pulses, Marine Propeller, Propeller Performance in Waves, Propeller Design, twin podded propulsion

## List of Variables

|           |                             |
|-----------|-----------------------------|
| $A$       | Wave amplitude              |
| $C_p$     | Pressure coefficient        |
| $D$       | Propeller diameter          |
| $J$       | Advance coefficient         |
| $K_T$     | Thrust coefficient          |
| $K_Q$     | Torque coefficient          |
| $L$       | Ship Length                 |
| $P_0$     | Atmospheric pressure        |
| $P_v$     | Vapour pressure of water    |
| $R$       | Propeller radius            |
| $T$       | Wave encounter period       |
| dB        | Sound level                 |
| $g$       | Acceleration due to gravity |
| $h$       | Depth of propeller shaft    |
| $k$       | Wave number                 |
| $n$       | Propeller rps               |
| $t$       | Time                        |
| $\Gamma$  | Blade tip circulation       |
| $\sigma$  | Cavitation number           |
| $\eta$    | Total propeller efficiency  |
| $\eta_0$  | Openwater efficiency        |
| $\rho$    | Water density               |
| $\lambda$ | Wavelength                  |

## 1. Introduction

Currently, there is growing demand in the industry to optimize ships for actual operating conditions rather than calm water conditions due to environmental concerns and the competition in the shipbuilding industry. Propeller designs, which are traditionally optimized in calm water, should be revisited to explore the possibility of performance improvement by optimizing them for operating in waves.

Propellers are usually designed using wake field and propulsion factors obtained in calm water condition. However, Moor *et al.* [1] found that the propulsion factors change in the presence of waves, a finding supported by many other studies[2-5]. Nakamura *et al.* [2] demonstrated that wake increases in the presence of waves due to pitching motion of the ship. Similar results, confirming substantial wake variation in waves were obtained in the RANS simulation carried out by Guo *et al.* [3]. Hayashi [6] observed the strong variation of wake in three different head waves using a model of KVLCC2 ship through PIV measurements. Chevalier *et al.* [7], Jessup *et al.* [8] studied the effect of waves on the cavitation inception of propeller operating in a seaway. A drop in the cavitation inception speed of the vessel was observed in the presence of waves.

Due to increasing demand for efficiency, it is no longer common to design propellers completely without cavitation. While allowing some cavitation to increase the efficiency, one should carefully avoid the detrimental effects of cavitation i.e. excessive pressure pulses and erosion. Pressure pulses generated due to cavitation can cause vibrations in the ship structure, thus affecting passenger comfort and in severe cases damage the hull structure. In merchant ships, bearing forces cause about 10% of propeller-induced vibration velocities, whereas pressure fluctuations or hull surface forces are responsible for approximately 90% of the vibrations [9]. Out of 47 ships surveyed for vibration problems, high pressure pulses were the source of the vibration problem in 80% of the cases. Cracks were also reported in the aft peak of 20 ships, which correlated with the amplitude of pressure pulses at blade pass frequency [10].

Propellers are normally wake adapted to achieve high efficiency while limiting the level of pressure pulses. Since it is found that operation in waves has a strong influence on the wake field [2-4], the performance of the propeller in the presence of waves should also be considered in the design process. Taskar *et al.* [11] performed one such investigation using KVLCC2 as a case vessel to study the effect of waves on cavitation and pressure pulses. Wake variations in three different head waves were considered for the analysis and a considerable increase in pressure pulses was observed in the presence of waves. Among various factors studied, wake variation had by far the largest influence on the pressure pulses. The study reports the need to analyze different types of ships to draw more generalized conclusions about the importance of waves. For single screw ships with high block coefficient like KVLCC2, the wake is considerably affected by the presence of hull, while for twin-screw or twin podded vessels wake is less disturbed by the hull. Thus, it can be expected that the effect of waves on wake distribution will be less pronounced in these cases. Therefore, to check the extent to which twin podded propulsion gets affected by waves, an 8000 dwt chemical tanker with twin Azipull thrusters was chosen for this study.

Considering that the lowering of pressure pulses comes at the expense of efficiency, accurate estimation of pressure pulses in realistic operating conditions can help in maximizing the propeller efficiency while still keeping pressure pulses within acceptable limits also when operating in waves.

Effect of various factors affecting propeller performance in waves like wake change, ship motions, wave dynamic pressure, added resistance and RPM fluctuation is studied. Cavitation and pressure pulses are calculated in different wave conditions and compared with the cavitation and pressure pulses in calm water wake.

## 2. Methods and validation

### 2.1. Propeller Analysis Tools

The propeller design software PropCalc, used by Rolls-Royce, has been utilized. The propeller analysis in PropCalc is performed by the software MPuF-3A, which is based on vortex lattice theory [12]. Details about the propeller geometry are given in Table 1. The open-water thrust, torque, and efficiency obtained from MPuF-3A computations is compared with the data from the propeller open water tests, which were carried out in the towing tank of MARINTEK using a model propeller of diameter 199.15 mm. The comparison can be seen in Figure 1. There is a slight discrepancy in the thrust and torque coefficients at lower J values, which could be due to the well-known limitations of potential theory based calculations at high angles of attack. In addition, the pod was located downstream of the propeller in the experiments whilst the presence of pod is not included in MPuF calculations.

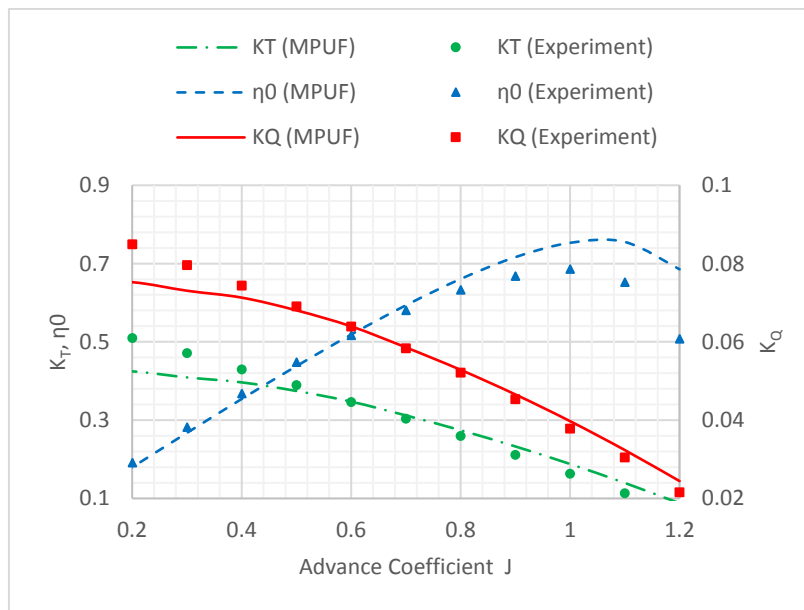


Figure 1 Comparison of MPuF-3A simulations with the experimental data for open water condition.

Table 1 Propeller Geometry

|                        |       |
|------------------------|-------|
| Diameter (D) (m)       | 3.3   |
| No of blades           | 4     |
| Hub diameter (m)       | 0.89  |
| Rotational speed (RPM) | 166   |
| $A_e/A_0$              | 0.435 |
| $(P/D)_{0.7}$          | 1.2   |
| Skew ( $^\circ$ )      | 18.6  |
| Rake ( $^\circ$ )      | -10   |

## 2.2. Wake Data in the presence of Waves

The wake is normally determined only for the calm water condition; therefore, availability of wake data in waves is the major hurdle in analyzing the propeller in the presence of waves. Experimentally obtaining the model wake data in waves would need specialized equipment like PIV (Particle Image Velocimetry) in the towing tank. CFD simulations in the presence of waves are also computationally expensive. However, with increasing hardware capacity and software developments, such calculations are becoming increasingly viable. Results from the Tokyo workshop [13] show that reliable results can be achieved for ship motions in the presence of waves using different CFD software. Note that for the ship, propelled by twin pods, the flow around the hull is expected to be less complex than with single screw ships where accurate predictions of, for example, bilge vortices are difficult. Therefore, the wake field, in this case, is also expected to be less demanding to predict compared with single screw ships.

Wake scaling issues can be avoided by simulating the full-scale ship in waves, which is certainly an advantage over model tests. Therefore, we decided to simulate the 8000 dwt chemical tanker in the presence of three different head waves at full-scale Reynolds number. Wavelengths were chosen such that different parts of the pitch RAO (response amplitude operator) can be covered, as wake is substantially affected by ship motions [11]. Simulations were performed at the design speed of the ship, which is 14

knots. The propeller was not included in the simulations, so only the nominal wake field was obtained. However, the pod was considered as a part of ship geometry and included in the computations, so that the effect of the pod on the wake variation was included. The ship main particulars are found in Table 2. The three different simulated conditions are specified in Table 3.

*Table 2 Ship Particulars*

|                                     |        |
|-------------------------------------|--------|
| Length between perpendiculars (m)   | 113.2  |
| Length at water line (m)            | 117.2  |
| Length overall (m)                  | 118.3  |
| Breadth at water line (m)           | 19     |
| Depth (m)                           | 15     |
| Draft (m)                           | 7.2    |
| Displacement (m <sup>3</sup> )      | 11546  |
| Block coefficient (C <sub>B</sub> ) | 0.7456 |
| Design Speed (knots)                | 14     |

*Table 3 Simulations Conditions*

| Ship speed [knot] | Froude number [-] | Wave amplitude [m] | $\lambda/L$ [-] | Encounter period [sec] |
|-------------------|-------------------|--------------------|-----------------|------------------------|
|                   |                   | 1.53               | 0.6             | 7.55                   |
| 14                | 0.212             | 1.28               | 1.1             | 5.89                   |
|                   |                   | 1.23               | 1.6             | 3.88                   |

### CFD modeling

Hydrodynamic ship simulations in waves with effect of viscosity included is not yet common practice at the design stage, since the viscosity is considered unimportant for ship motions in waves and because it is considered too computationally demanding and time-consuming to apply these methods to a time

constrained design loop. In this case, the aim of the simulations was primarily to obtain wake change in the presence of waves, in which case the effect of viscosity is essential.

All simulations were performed in full scale using an Unsteady Reynolds Averaged Navier-Stokes, URANS, solver Star-CCM+, where the SST  $k-\omega$  model was used for turbulence closure. An all- $y^+$  wall treatment function was assigned to deal with the near-wall flow. The  $y^+$ -target was of the order of 50-80. A Volume of Fluid, VOF, multiphase model was employed to calculate the flow motion in the two fluid phases, air and sea water. The waves were generated with a 5<sup>th</sup> order approximation to the Stokes theory of waves. The response and motion of the ship in waves was managed by a Dynamic Fluid Body Interaction, DFBI, model. The motion of the ship was constrained to two degrees of freedom, heave and pitch. As for domain size, it is preferable to use as small domain as possible to minimize the cell count. However, it is also important to make sure that the boundaries of the domain are not so close that they can reflect back non-physical waves into the domain. According to [11], it is recommended that the inlet boundary should be located 1-2 ship lengths upstream of the hull and outlet boundary should be 3-5 ship lengths downstream to avoid any reflections from the boundary walls. Domain size used for the simulations can be seen in Figure 2. The computational domain was discretized by a predominantly hexahedral mesh with anisotropic mesh refinement. 80 cells per wavelength and 20 per wave amplitude resolve the wave zone. An overset mesh domain handles the ship motion with respect to the mesh. Details about the cell count and the number of cells in the background and overset mesh can be seen in Table 4. Surface mesh on the hull in the bow and stern region can be seen in Figure 3 and Figure 4 respectively. Overset and background mesh in the domain can be seen in Figure 5 and Figure 6. A refinement to capture diverging waves can be observed in Figure 6.



Table 4 Cell count for simulations in waves (in Million)

| $\lambda/L$ | Background | Overset | Total |
|-------------|------------|---------|-------|
| 0.6         | 34.4       | 9.7     | 44.1  |
| 1.1         | 32.0       | 14.9    | 46.9  |
| 1.6         | 20.6       | 19.8    | 40.4  |

In a zone at the exit of the domain, waves are numerically damped out to minimize reflections. All simulations were performed with half of the hull along with symmetry boundary condition on the vertical plane going through the center of the ship. No slip condition was applied on the surface of the hull. A pressure outlet was used on the downstream boundary. On the rest of the boundaries, a velocity inlet condition was applied. The time step for the solver is set so that it fulfills the criteria needed to transport the wave through the domain maintaining a sharp air-water interface. It was also necessary to limit the time step due to the motion of the ship, and in all cases this criterion was limiting the time step. 2<sup>nd</sup> order numerical schemes were used for all flow equations as well as for time discretization.

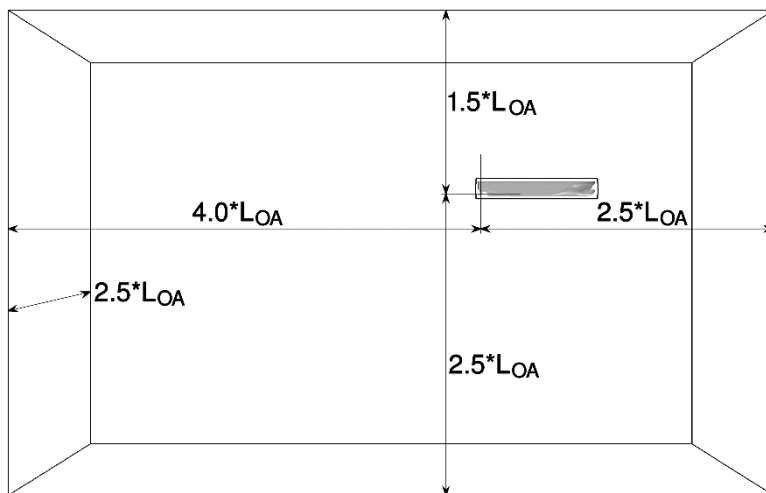
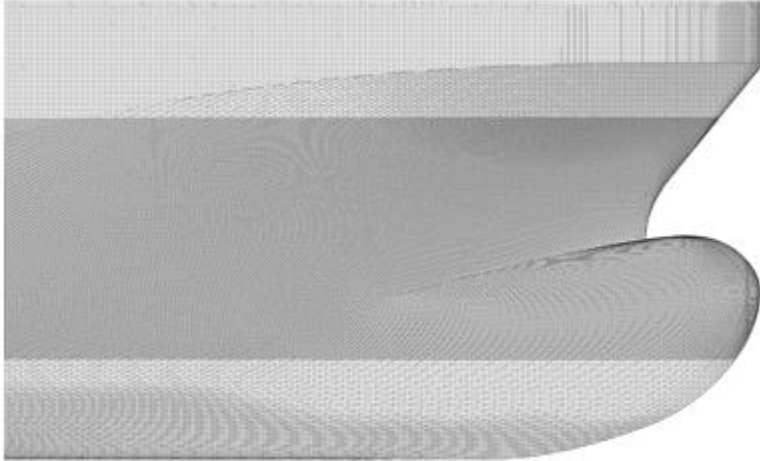
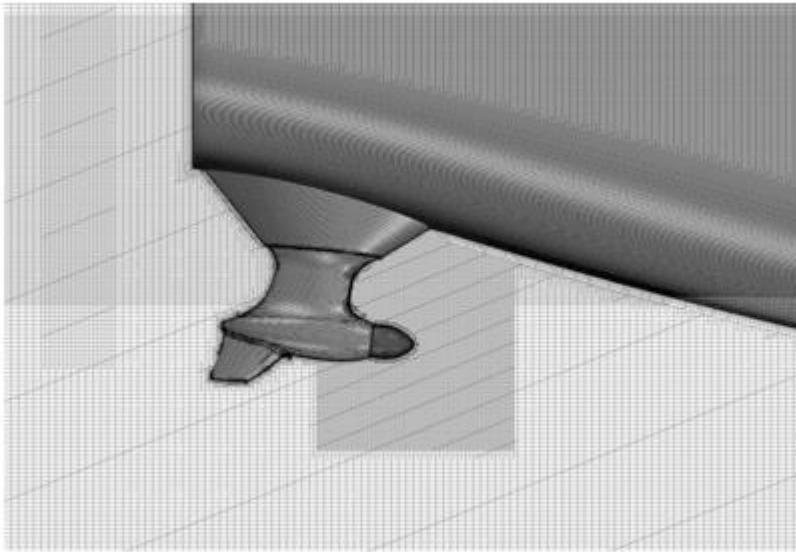


Figure 2 Simulation domain and boundaries.



*Figure 3 Surface mesh around bow region of the ship.*



*Figure 4 Surface mesh around the stern and pod of the ship.*

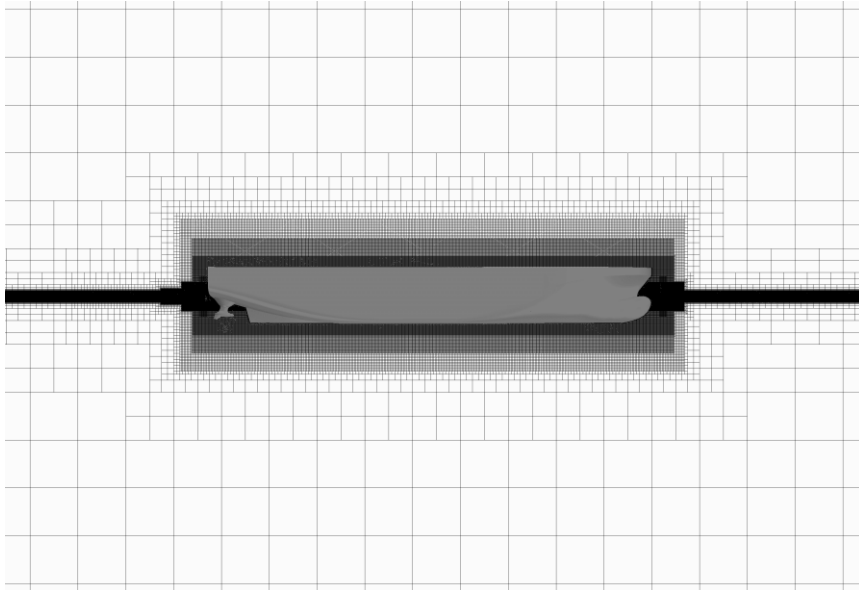


*Figure 5 Vertical cross section of mesh in the simulation domain.*

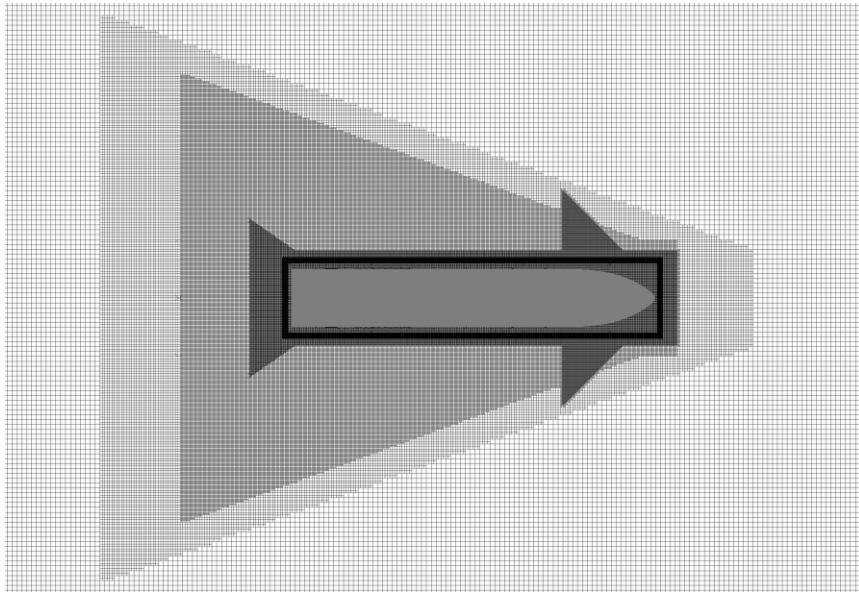


*Figure 6 Horizontal cross section of mesh in the simulation domain.*

## Validation

CFD simulations were also run in calm water with the same mesh settings as in the presence of waves.

Ship resistance, sinkage, and trim were compared with the experimental values from the model tests [14].

CFD computations show a good match with the full-scale predictions obtained using model tests.

Table 5 Comparison of results in calm water

|             | Experiment | CFD    |
|-------------|------------|--------|
| Drag [kN]   | 207.05     | 210.8  |
| Sinkage [m] | 0.148      | 0.137  |
| Trim [deg]  | -0.23      | -0.264 |

To validate the CFD computations in waves, ship motions obtained from the simulations were compared with motion RAOs (Response amplitude operators) obtained from potential flow calculations as well as available experimental results. Ship motion RAOs were calculated using linear strip theory, implemented in the ShipX Veres software [15]. Seakeeping tests were performed at MARINTEK [16] using the scaled model of 1:16.57. Heave and pitch were measured in the presence of waves corresponding to the full-scale wave amplitude of 1m. Comparison of heave and pitch motions, in terms of Response Amplitude Operators (RAO) obtained from CFD, ShipX Veres and experiments are presented in Figure 7 and Figure 8. Ship motions obtained from CFD simulations show a fairly good match with the experimental results and potential flow simulations. Propeller ventilation due to limited submergence is a common problem for ships operating in high waves. In the current case, the calm water submergence ratio was  $h/R=3$ , where  $h$  is submergence of the propeller shaft and  $R$  is the propeller radius, while the minimum propeller submergence in waves was  $h/R=2$ . Therefore, propeller ventilation is not considered to be a problem here and not further considered in this study.

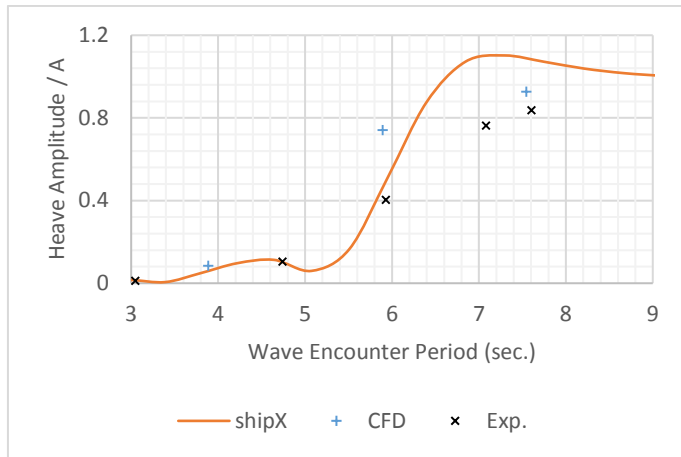


Figure 7 Comparison of heave motion response using CFD, experiments, and ShipX calculations.

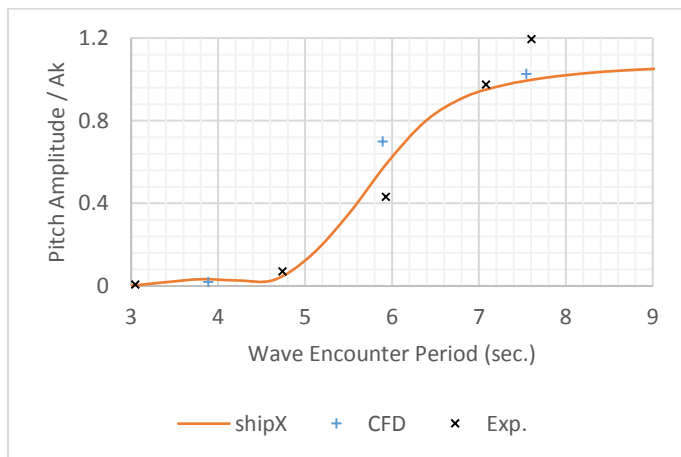


Figure 8 Comparison of pitch motion response using CFD, experiments, and ShipX calculations.

### CFD Results

The aim of the CFD computations was to obtain the wake in the presence of waves. Wake data was extracted from the simulation after ship motions had stabilized in the computations. Wake data obtained in the presence of three different head waves are presented in Figure 9, Figure 10 and Figure 11. Even for the ship with twin azimuthal propulsion, where the effect of the hull on wake distribution is lower than that compared to the single screw ship, the presence of waves seems to have a significant impact.

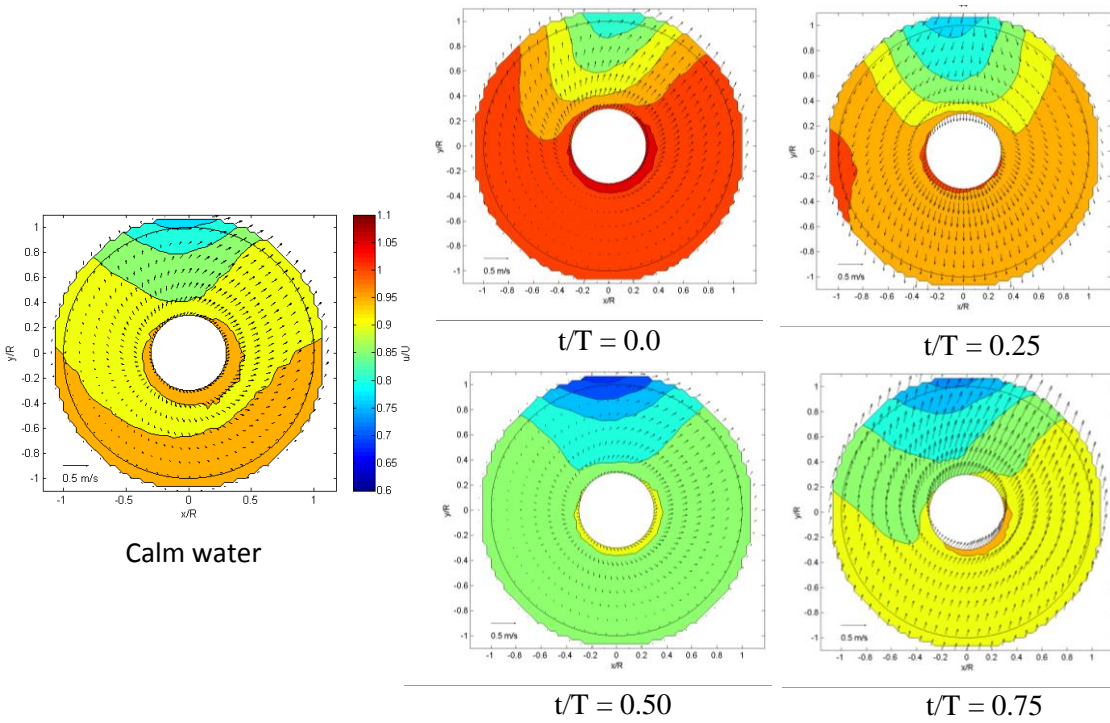


Figure 9 Wake in calm water compared to the wake in the presence of wave having wavelength ratio  $\lambda/L = 1.6$ .

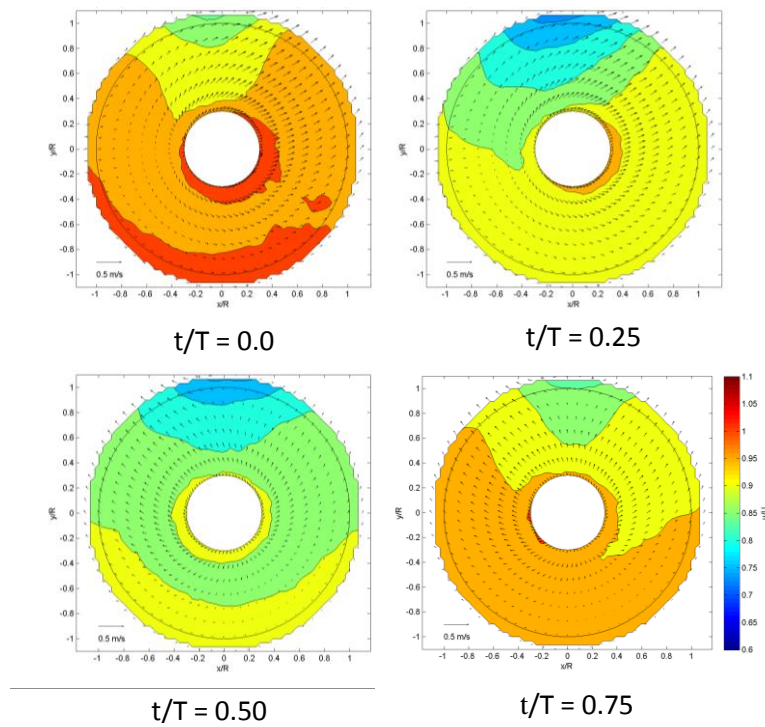


Figure 10 Wake in the presence of wave having wavelength ratio  $\lambda/L = 0.6$ .

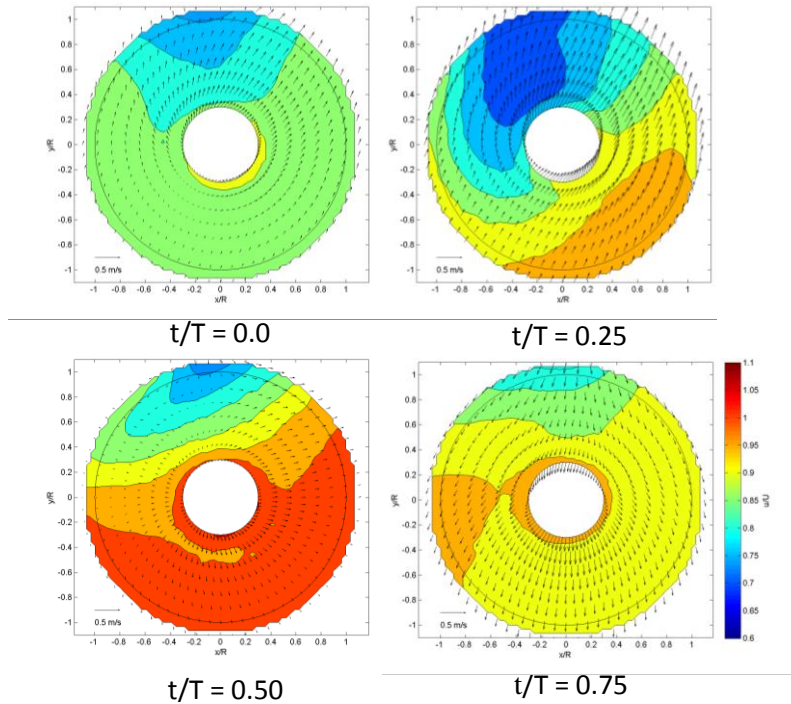


Figure 11 Wake in the presence of wave having wavelength ratio  $\lambda/L = 1.1$ .

### 2.3. Calculation of speed loss

Self-propulsion tests were performed at MARINTEK [16] for the case vessel considered in this paper. Speed loss was calculated in the presence of regular as well as irregular waves. Irregular waves were created using a JONSWAP spectrum with the value of the peakedness function ( $\gamma$ ) equal to 3.3. In the presence of irregular waves with significant waveheight 2m and peak period of 8.8 seconds, ship speed reduced by 1 knot at constant power setting. Speed loss was 3 knots for 4m significant waveheight and 11 seconds peak period. Since CFD simulations were performed at regular wave amplitudes ranging from 1.23m to 1.53m, it would have been appropriate to consider speed loss in the waves corresponding to 3m significant waveheight. In the absence of experimental data in this particular condition, propeller cavitation and pressure pulses were calculated at both 12 and 13 knots, which corresponds to 1 and 2 knots of speed loss. Irregular waves were considered for the calculation of speed loss to avoid getting



unrealistically low ship speeds since added resistance in regular waves is often much larger than that in irregular waves.

#### 2.4. Calculation of propeller RPM fluctuation

Engine load fluctuates due to time varying wake in waves, which leads to fluctuations in the engine RPM. The amount of fluctuation depends on the inertia of engine, propeller and shaft, control system and the wake variation [17]. In the absence of engine-propeller model for the propulsion system of this particular vessel, the amount of RPM fluctuation has to be approximated. This approximation is done by computing the change of torque due to the change of wake in waves, keeping RPM constant. Then, the change in RPM needed to produce the same change in torque is determined keeping wake constant.

In order to validate this methodology, the case of KVLCC2 was considered. Torque variations due to wake variation were taken from [18] to calculate RPM fluctuations using the method described above. Results were compared with RPM fluctuations calculated in [17] using engine-propeller coupled model. The above method predicts 4% fluctuations in RPM whereas fluctuations using engine-propeller coupled model are close to 3%. Thus, it is concluded that the approximate method to calculate RPM fluctuations used here gives slightly conservative results.

Applying this method to the current case vessel, propeller RPM was found to fluctuate by 2.4%, 4.2% and 3% in  $\lambda/L = 0.6, 1.1$  and  $1.6$  respectively. Therefore, the propeller was analyzed at maximum RPMs i.e. 170, 173 and 170 RPM, which correspond to an instant of highest average wake velocity (at  $t/T = 0, 0.51$  and  $0$ ) in  $\lambda/L = 0.6, 1.1$  and  $1.6$  respectively. Simulations reported in [17] show that the RPM fluctuates in phase with the average wake velocity meaning that RPM is largest when the average propeller inflow is largest. Although the current vessel and the propulsion system is much different from the one used by Taskar *et al.* [17], this conclusion can still be valid, since wake varies much slower than the propeller RPM. Hence the



changes due to wake variation can be assumed to be quasi-steady from the propulsion system point of view.

### 2.5. Pressure Pulse calculation

Pressure pulses have been calculated using HullFPP [19]. The time history of cavity volume variation, obtained from unsteady propeller calculations in MPuF-3A, is used to derive field point potential induced by the cavitating propeller. The diffraction potential on the hull is solved using a potential theory based boundary element method to obtain the solid boundary factor. The fluctuating pressure on the hull is then determined by multiplying free-space pressures by the solid boundary factor. Pressure pulse calculations using HullFPP have been compared with experimental results by Hwang *et al.* [20]. In the current analysis, pressure pulses were computed on a flat plate at a distance of 30% of the propeller diameter from the blade tip.

### 2.6. Calculation of unsteady wave pressure

Ship motions affect the propeller submergence and therefore the hydrostatic pressure at the propeller, and passing waves can alter the ambient pressure around the propeller. Both effects influence the cavitation. The total pressure was calculated at the location of the propeller shaft, considering propeller submergence as well as dynamic wave pressure. Propeller submergence was calculated based on heave, pitch, and wave elevation. The phase of the passing wave was considered for the calculation of dynamic wave pressure. The total pressure thus obtained was converted to effective propeller immersion in calm water condition.

## 3. Analysis

The aim of this study is to find out the effect of waves on cavitation and pressure pulses due to waves and ship motions. Therefore, the effect of different factors affecting the propeller performance was studied.

Variation in cavitation and pressure pulses was analyzed due to the influence of wake variation, ship motions, RPM fluctuations and speed loss due to added resistance. Each of these factors was separately studied to calculate their order of importance on the propeller performance so that the factors affecting the most can be taken into account while designing the propellers. The effect of each factor is studied in the following sections.

### 3.1. Effect of wake variation and change in cavitation number

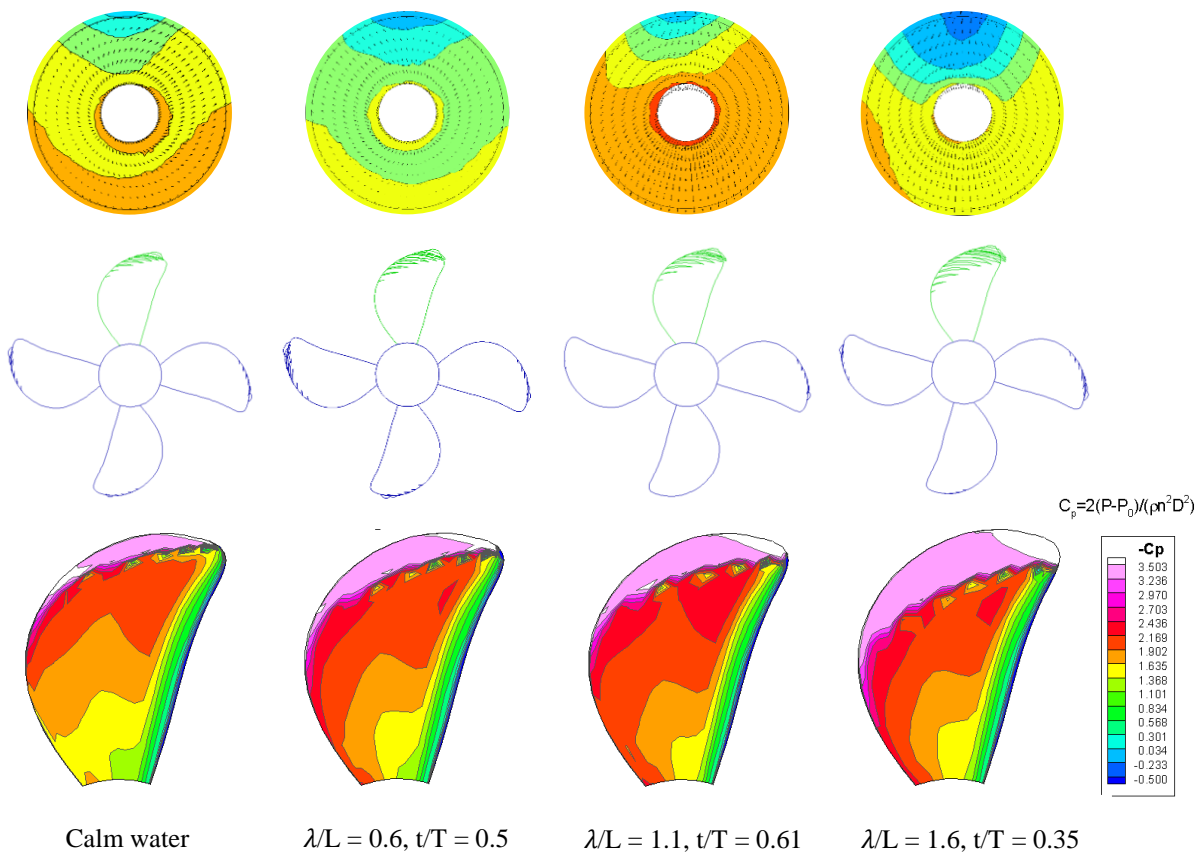


Figure 12 Maximum suction side cavitation seen in each wavelength considering only wake change compared to cavitation in calm water wake.

The propeller was analyzed in calm water and at different times in each wave condition. The wake was assumed quasi-steady for the analysis; since the frequency of propeller rotation is much larger than the

encounter frequency of waves. In the analysis, propeller depth was kept constant even in the presence of waves to separately observe the effect of wake change.

Propeller cavitation and pressure distribution on the blade at 12 O'clock position is presented in Figure 12 at the instant of maximum cavitation in each wave condition. In all cases, the maximum cavitation is seen at 12 O'clock position of the propeller blade and it is larger than the cavitation in the calm water wake. This difference in the amount of cavitation is due to wake variation as wake varies considerably in waves. Among three wave conditions  $\lambda/L=1.6$  causes a maximum increase in the amount of cavitation followed by  $\lambda/L=1.1$  and 0.6 respectively. Also, note that in addition to the cavitation at 12 O'clock blade position, the cavitation volumes seen at other blade locations also vary substantially due to wake variation. Therefore, not just the volume but the pattern of cavitation volume variation with respect to the blade position gets affected due to wake change in waves. Substantial variation in the pressure distribution on the propeller blade can be observed. Especially close to leading edge of the blade,  $-C_p$  is higher in waves than that in calm water wake.

The maximum cavitation occurs at a single instance in time. Therefore, to visualize the variation of cavitation patterns the propeller goes through in one wave encounter period, the minimum cavitation at 12 O'clock position in each case is shown in Figure 13. The minimum cavitation in  $\lambda/L=1.1$  and 1.6 is comparable to the cavitation in calm water wake however in  $\lambda/L=0.6$  it is lower than in calm water. Therefore, in  $\lambda/L=1.1$  and 1.6 average cavitation on propeller blades over one wave encounter period is larger than the cavitation volume in calm water. Pressure distribution in calm water and  $\lambda/L=1.6$  is almost identical. Whereas in  $\lambda/L=0.6$  and 1.1, the distribution of  $-C_p$  is similar and less severe as compared to the calm water case.

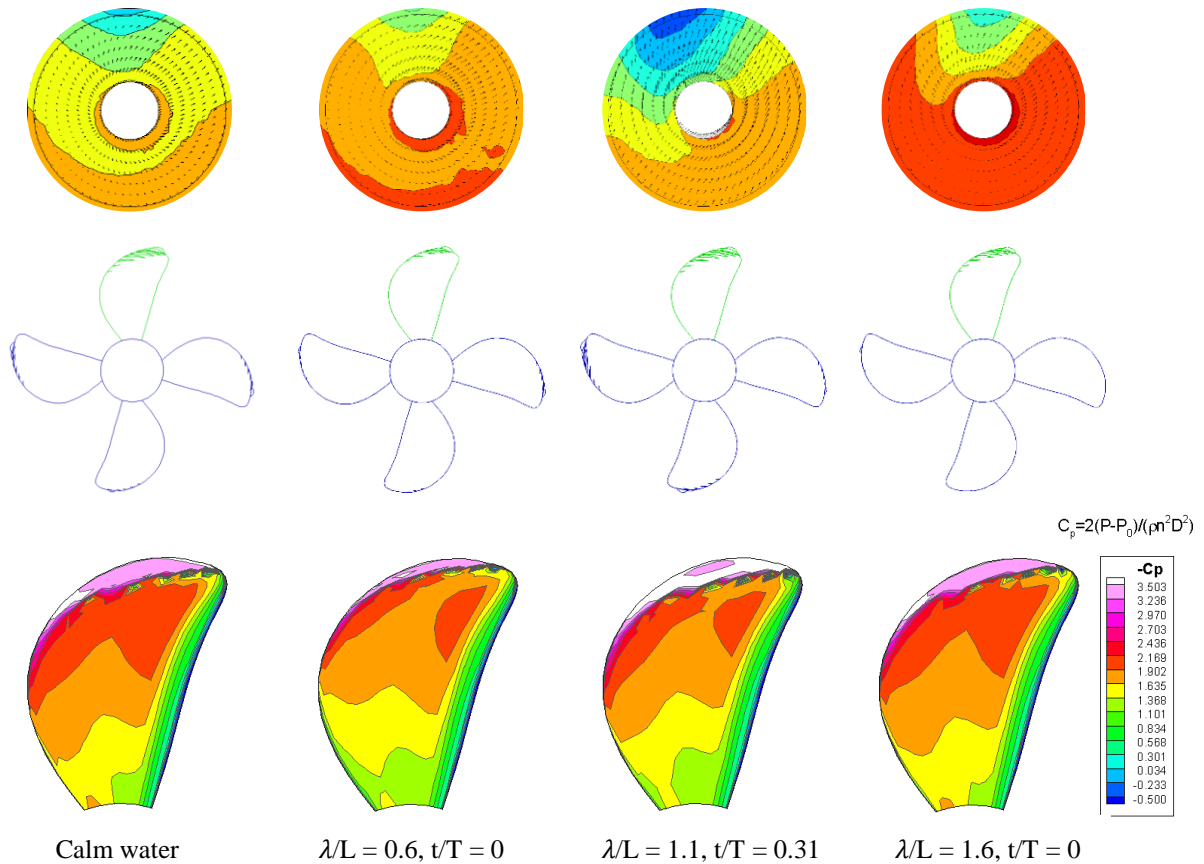


Figure 13 Minimum suction side cavitation seen in the presence of wave among all three waves considering only wake change.

In addition to the wake change, propeller immersion varies in waves due to ship motion, leading to a change in ambient pressure. Therefore, the propeller was analyzed in different wake fields taking into consideration the effect of ship motions and wave dynamic pressure by changing effective propeller immersion. Unlike in the earlier case, the cavitation number was varied along with the wake variation. The maximum cavitation in each wave condition is shown in Figure 14. Comparing Figure 14 with Figure 12, the maximum cavitation decreases in  $\lambda/L=1.6$ . However, it increases in the other two cases. Therefore, in  $\lambda/L=1.6$  the wake distribution corresponding to the maximum cavitation occurs at higher cavitation number due to the presence of waves whereas the opposite is true for  $\lambda/L=0.6$  and 1.1. After considering the effect of varying propeller submergence, the maximum cavitation occurs at the same time instant in  $\lambda/L=1.1$  and 1.6, while in  $\lambda/L=0.6$  it is seen at a different time instant.

Cavitation number is defined as follows:

$$\sigma = \frac{P_0 + \rho gh - P_v}{0.5 \rho n^2 D^2}$$

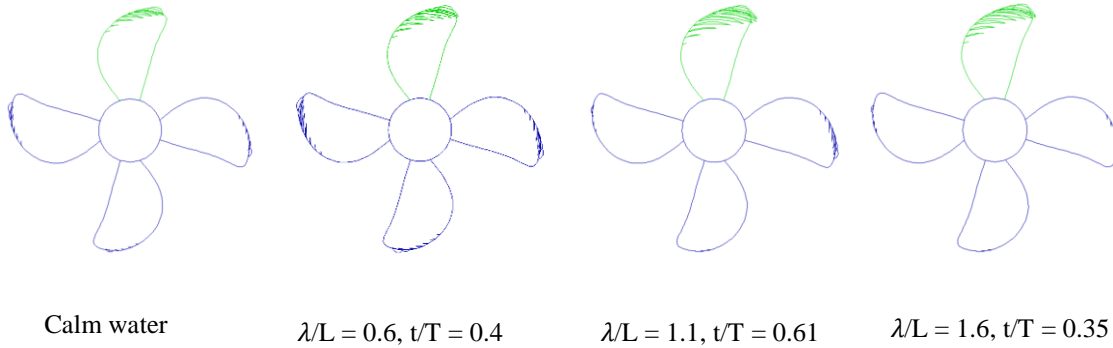


Figure 14 Maximum suction side cavitation seen in each wave considering wake change, ship motions, and dynamic wave pressure.

To study the variation of cavitation with respect to blade angle at different time instances, cavitation volumes have been plotted as function of blade angle in calm water and waves with and without varying the cavitation number. Cavity volume variations at fixed cavitation number in regular head waves  $\lambda/L=0.6$ , 1.1 and 1.6 can be seen in Figure 15, Figure 16 and Figure 17 respectively. In  $\lambda/L=0.6$ , the maximum cavitation volume is lower than that in calm water wake for most of the time. In  $\lambda/L=1.1$  and 1.6, larger variations in cavity volume over a wave-passage, as well as cavity volume variation at different blade angles are found. In  $\lambda/L=1.6$  cavity volume variations are far greater than for the other two cases. The maximum cavitation volumes in  $\lambda/L=0.6$ , 1.1 and 1.6 are higher than those in calm water by 28%, 68%, and 202% respectively. That means in  $\lambda/L=1.6$ , maximum cavitation volume reaches almost three times the cavitation volume seen in calm water wake. Additionally, in some of the cases, the cavity volume varies in a different way than in calm water wake ( $\lambda/L=1.1$ ,  $t/T=0.1$ ;  $\lambda/L=1.6$ ,  $t/T=0.59$ ). As the cavitation number has been kept constant in these simulations, the effect is only due to wake variation. Therefore, from the cavitation point of view, wake in wavelength  $\lambda/L=1.6$  is most critical, followed by  $\lambda/L=1.1$  and 0.6. Interestingly, heave and pitch motions are largest in  $\lambda/L=1.6$  followed by  $\lambda/L=1.1$  and 0.6, which suggests that the ship motions are

important for wake variations. The difference between thrust and torque coefficients considering cavitating and non-cavitating propeller calculations was insignificant in spite of large increase in cavity volumes. This means that even if cavity volumes increase significantly due to waves, they are not large enough to affect the thrust and torque.

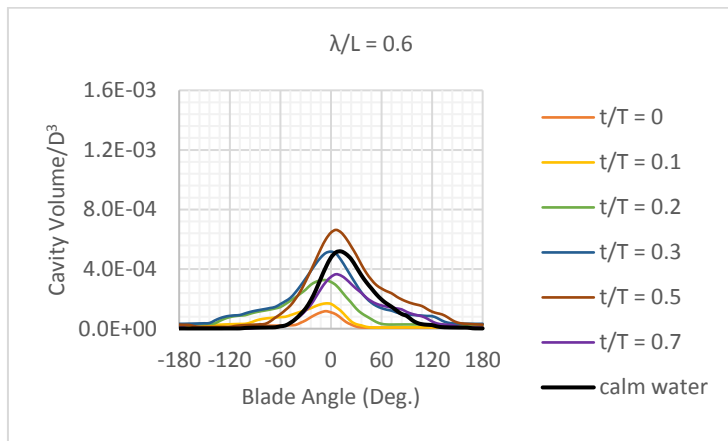


Figure 15 Cavity volume variation in  $\lambda/L = 0.6$  at different times due to wake variation.

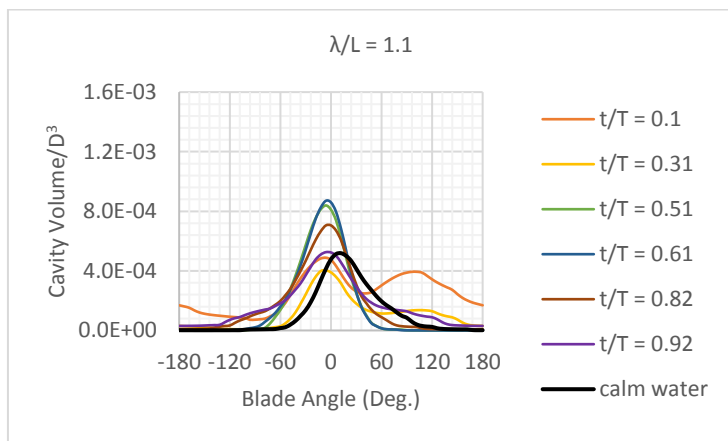


Figure 16 Cavity volume variation in  $\lambda/L = 1.1$  at different times due to wake variation.

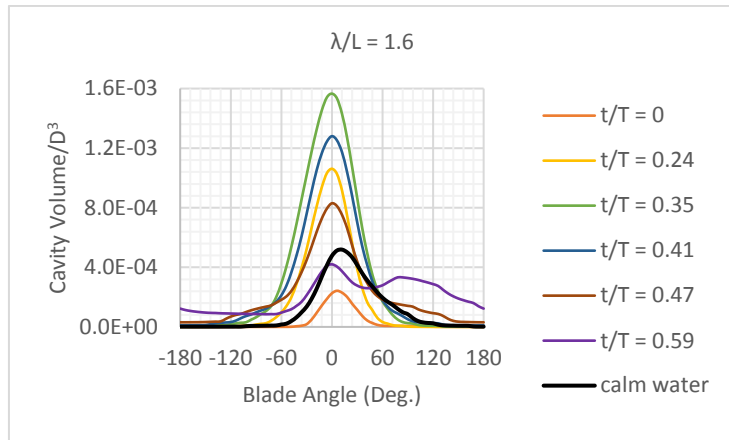


Figure 17 Cavity volume variation in  $\lambda/L = 1.6$  at different times due to wake variation.

Cavity volume variation considering also the effect of a change in cavitation number in addition to the wake change is plotted in Figure 18, Figure 19 and Figure 20 for  $\lambda/L=0.6$ , 1.1 and 1.6 respectively. Comparing Figure 15, Figure 16 and Figure 17 with Figure 18, Figure 19 and Figure 20 respectively, the maximum cavitation volume is higher in  $\lambda/L=0.6$ , 1.1 and lower in  $\lambda/L=1.6$  when the cavitation number is varied along with the wake. After considering the effects of change in propeller immersion due to ship motions and wave dynamic pressure the maximum cavitation volume was higher than that in calm water by 42%, 148% and 135% in  $\lambda/L=0.6$ , 1.1 and 1.6 respectively. Therefore,  $\lambda/L=1.1$  turns out to be the critical operating condition as far as the cavitation volume is concerned.

Wake distributions leading to high cavitation in  $\lambda/L=1.6$  occur at higher propeller immersion whereas the opposite is true in the case of  $\lambda/L=1.1$  (Figure 21).

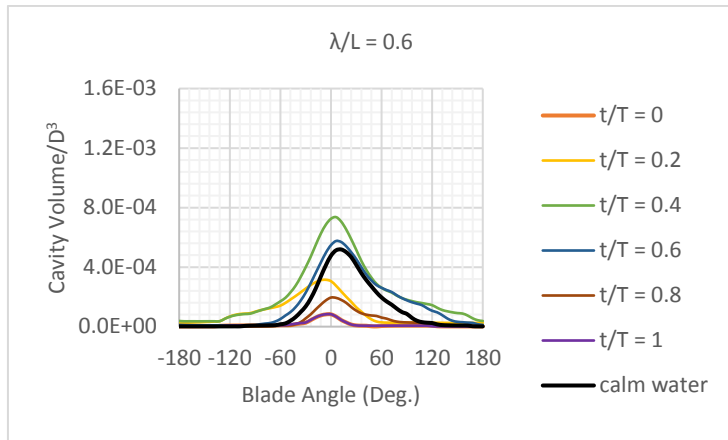


Figure 18 Cavity volume variation in  $\lambda/L = 0.6$  at different times due to wake variation, ship motions and dynamic wave pressure.

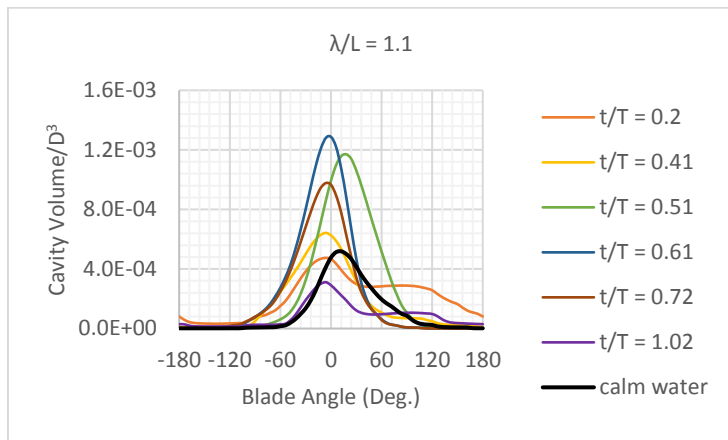


Figure 19 Cavity volume variation in  $\lambda/L = 1.1$  at different times due to wake variation, ship motions and dynamic wave pressure.

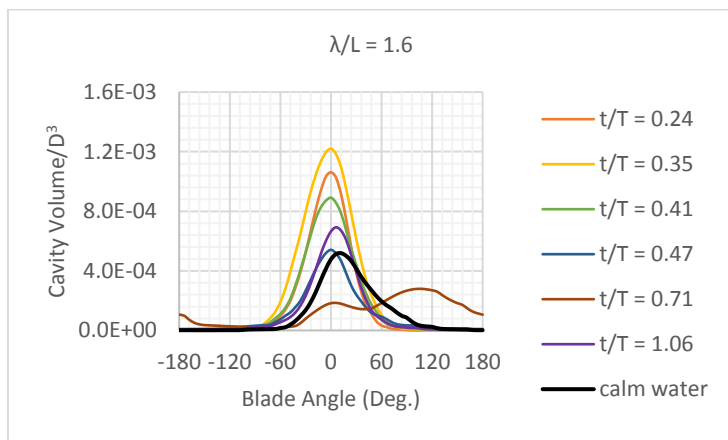


Figure 20 Cavity volume variation in  $\lambda/L = 1.6$  at different times due to wake variation, ship motions and dynamic wave pressure.



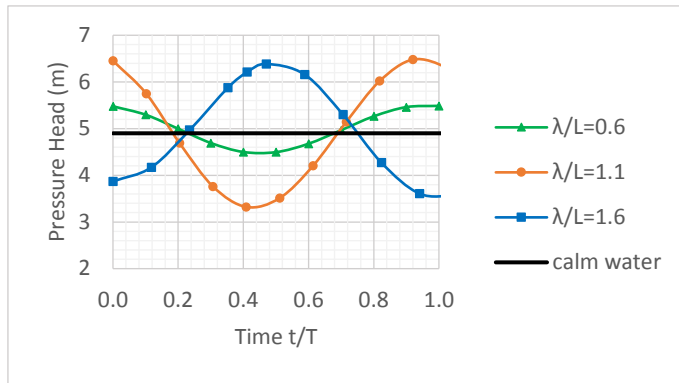


Figure 21 Variation in pressure head at the location of propeller shaft in the presence of waves.

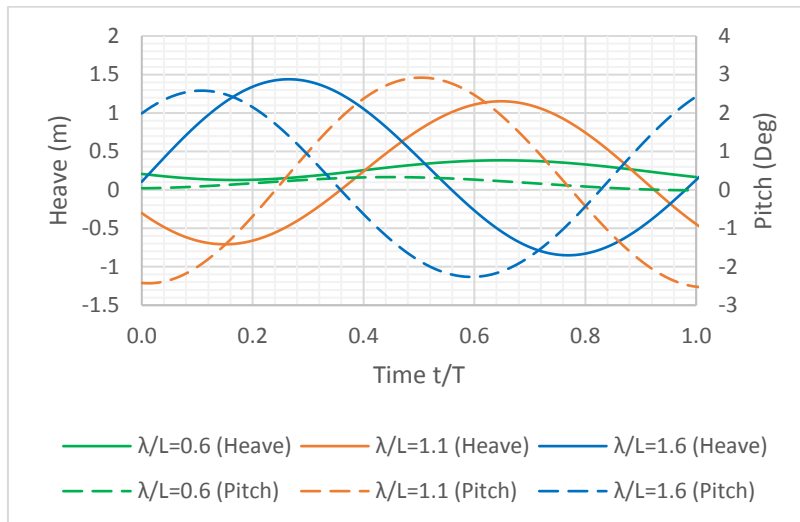


Figure 22 Phases of heave and pitch at different times in three waves. (Heave: downwards is positive; Pitch: bow down is positive)

Considerable cavity volume variation makes it necessary to investigate the level of pressure pulses in the presence of waves; since pressure pulses are proportional to the second derivative of cavity volume [21]. Pressure pulses were computed with and without considering the effect of a change in cavitation number due to ship motion and wave dynamic pressure. Pressure pulses in the first, second and third harmonic of blade pass frequency are plotted in Figure 23, Figure 24 and Figure 25 at fixed cavitation number. The first harmonic of blade pass frequency is usually the highest and the most important from the hull vibration point of view. All three harmonic amplitudes of pressure pulses are substantially higher in  $\lambda/L=1.1$  and  $1.6$  as compared to pressure pulses in calm water wake. In these two wave conditions, pressure pulses are higher than calm water pressure pulses for most of the wave encounter period; in fact, the minimum

pressure pulses are of similar magnitude as in calm water wake. This trend is consistent for all three harmonic amplitudes. Therefore, wake variation does significantly affect the propeller performance in the presence of waves.

Higher pressure pulses in  $\lambda/L=1.1$  and  $1.6$  correspond to the increase of wake peak in the nominal wake. Especially, the magnitude of the wake peak with respect to average wake seems to play an important role; which is as per the expectations [22]. Nominal wakes at the instances of high pressure pulses are such that the blade at 12 O'clock position experiences higher load as compared to the other blades as observed in Figure 12. Interestingly, maximum pressure pulses in  $\lambda/L=1.1$  and  $1.6$  correlate well with the phases of heave and pitch motions (from Figure 22 and Figure 23). Which means, in  $\lambda/L=1.1$ , maximum pressure pulses are seen close to  $t/T=0.6$  and heave motion is also maximum around  $t/T=0.6$ . Similar is true for  $\lambda/L=1.6$ .

Only in the case of  $\lambda/L=0.6$ , alteration in the level of pressure pulses is relatively small; the magnitude of pressure pulses fluctuates around the value in calm water wake. The increase in the cavitation volume is also comparatively small in this case as seen earlier. Therefore, wake change in  $\lambda/L=0.6$  has little effect on cavitation and pressure pulses.

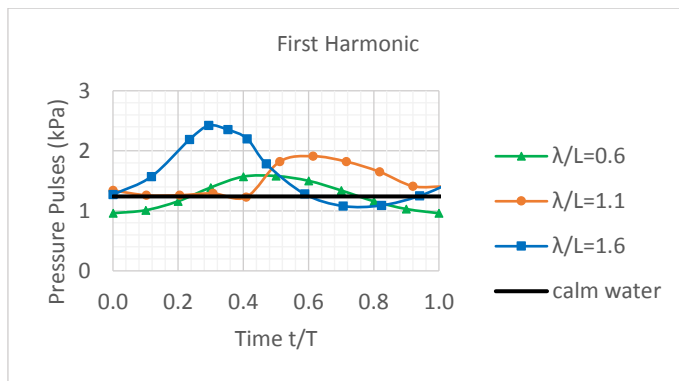


Figure 23 First harmonic amplitude of pressure pulses in waves considering wake variation.

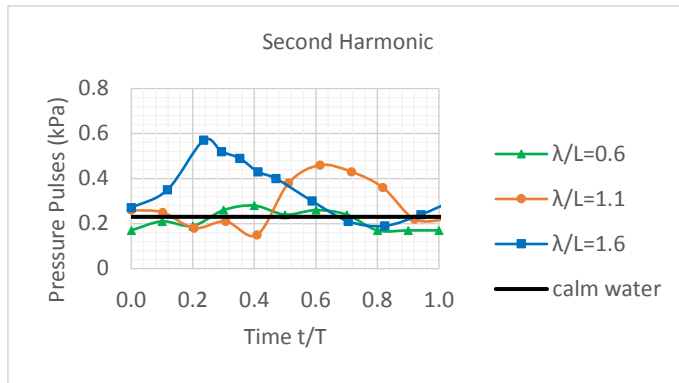


Figure 24 Second harmonic amplitude of pressure pulses in waves considering wake variation.

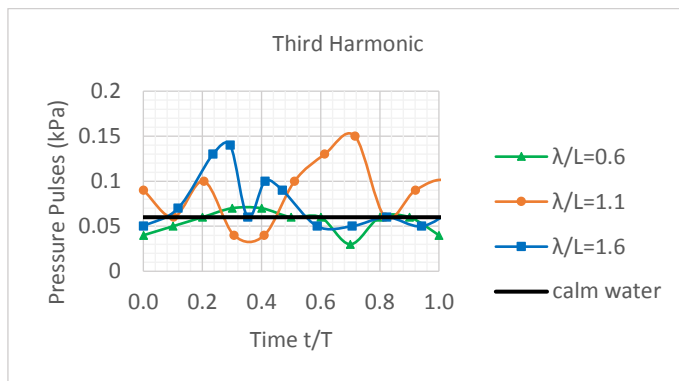


Figure 25 Third harmonic amplitude of pressure pulses in waves considering wake variation.

It is interesting to note that pressure pulses vary due to variation in wake distribution and not because of the change in average wake when ship motions are significant i.e. in  $\lambda/L = 1.1$  and  $1.6$ . Variation in Taylor wake fraction and variation of thrust and torque coefficient in the presence of waves are plotted in Figure 26 and Figure 27 respectively. Variation in Taylor wake fraction and pressure pulses is not synchronous except in the case of  $\lambda/L=0.6$ , where ship motions are much smaller than the other two cases, causing minor deviations in wake distribution. Therefore, in  $\lambda/L=0.6$  the first harmonic of pressure pulses vary due to average wake rather than wake distribution, since a clear correlation between wake fraction and first harmonic amplitude of pressure pulses is evident.

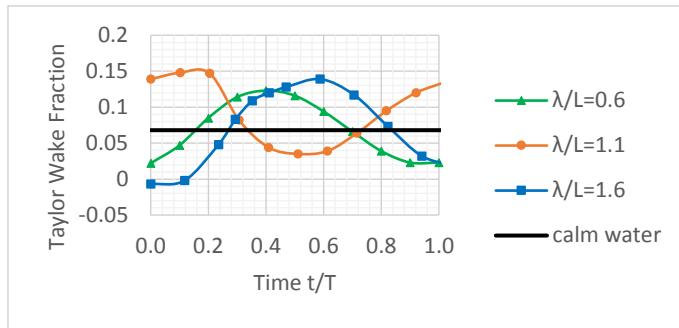


Figure 26 Average wake variation in waves.

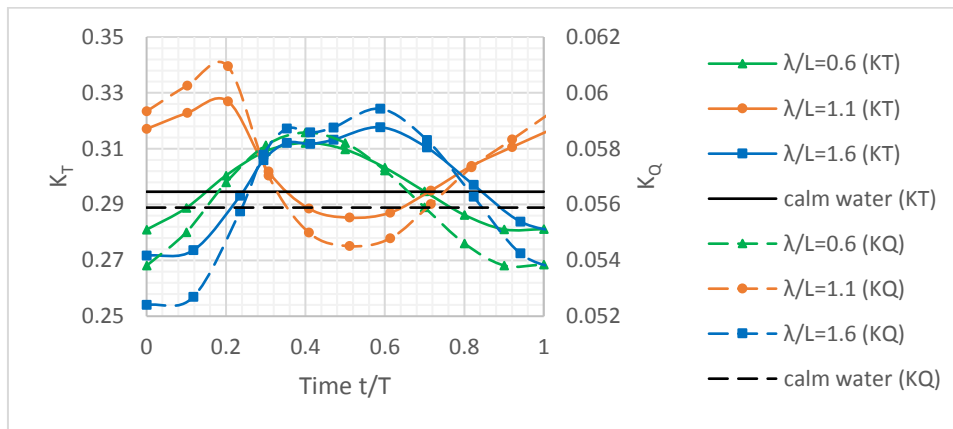


Figure 27 Variation of thrust and torque coefficient in the presence of waves due to wake variation

Pressure pulses considering the effect of a change in propeller immersion and the dynamic pressure due to wave are plotted in Figure 28, Figure 29 and Figure 30. As for cavitation volumes, maximum pressure pulses increase in  $\lambda/L=0.6$  and  $1.1$  after including variation in cavitation number, whereas they decrease in the case of  $\lambda/L=1.6$ . Still, the level of pressure pulses is significantly larger than the calm water pressure pulses in all three harmonic amplitudes except in the case of  $\lambda/L=0.6$ .

Pressure pulses created in  $\lambda/L=1.1$  and  $1.6$  are equally larger than that in calm water wake except in the case of third harmonic amplitude where pressure pulses are greater in  $\lambda/L=1.6$ . The first harmonic of pressure pulses in  $\lambda/L=0.6$ ,  $1.1$  and  $1.6$  increase at maximum by 30%, 81%, and 77% respectively. Second and third harmonic amplitudes are notably higher than those in calm water wake. Therefore, the combined effect of wake variation and change in cavitation number has a noteworthy influence on the level of pressure pulses.

To separate the effect of the varying cavitation number, the difference in the level of pressure pulses in Figure 28 and Figure 23 is plotted in Figure 31 with the corresponding change in propeller depth. Pressure pulses are also computed at different propeller depths in calm water wake. Propeller immersion is the effective depth of the propeller shaft such that the variation of cavitation number due to wave dynamic pressure is also taken into account. The rate of change of pressure pulses with respect to the propeller immersion is comparable in all cases. Calm water propeller immersion is 4.9m, which varies from 3.5m to 6.5m in the presence of waves, causing a corresponding change in pressure pulses ranging from 0.28 kPa to -0.28 kPa. Comparing Figure 31 with Figure 23 shows that the change in pressure pulses due to wake variation alone is much larger than the change of pressure pulses due to depth variation. Moreover, the effect of a change in propeller depth can be estimated by ship motions and the rate of change of pressure pulses by simulating the propeller in calm water wake at different immersions whereas considering the effect of wake variation is much more complicated.

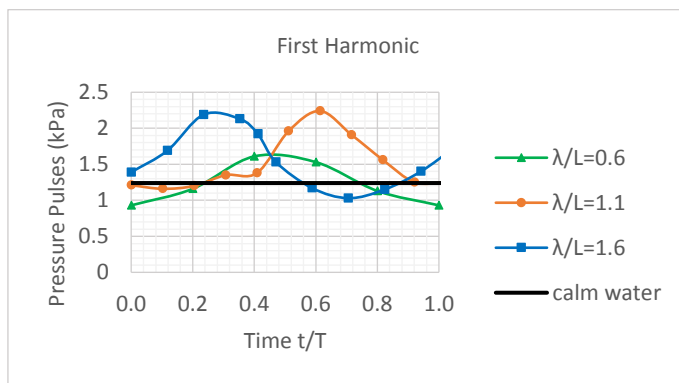


Figure 28 First harmonic amplitude of pressure pulses in waves considering wake variation, ship motions, and dynamic wave pressure.

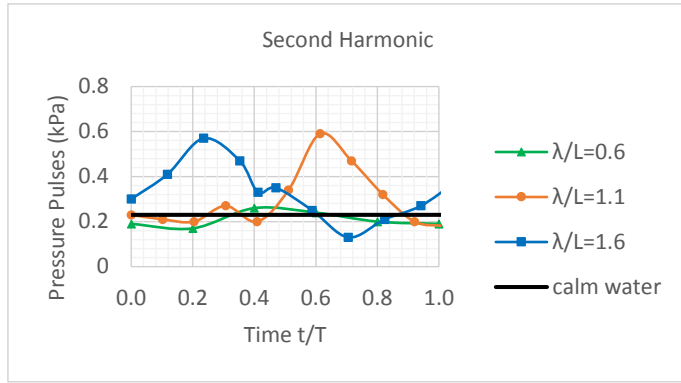


Figure 29 Second harmonic amplitude of pressure pulses in waves considering wake variation, ship motions, and dynamic wave pressure.

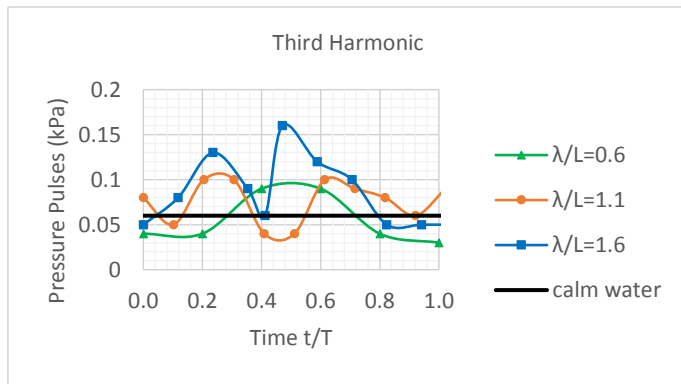


Figure 30 Third harmonic amplitude of pressure pulses in waves considering wake variation, ship motions, and dynamic wave pressure.

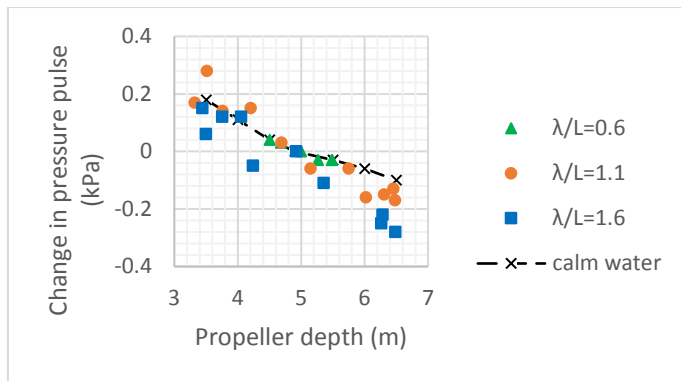


Figure 31 Variation in the first harmonic amplitude of pressure pulses due to change in effective propeller depth (Propeller immersion in calm water is 4.9m).

Pressure pulses of blade pass frequency and higher harmonics are often responsible for hull vibration and hull damage close to the propeller. However, noise created by the tip vortex has high frequency, and might cause inboard noise detrimental for crew and passenger comfort. Noise due to tip vortex can be estimated

using the tip vortex index (TVI) defined by Raestad [23]. Since TVI is a function of tip circulation, circulation at blade section  $r/R=0.997$  at 12 O'clock blade position is compared in the presence of waves at different time intervals. The variation in tip circulation can be seen in Figure 32, where a similar amount of increase in tip circulation is observed in  $\lambda/L=0.6$  and  $1.6$  while in  $\lambda/L=1.1$ , the variation is rather small. The maximum tip circulation in  $\lambda/L=0.6$  and  $1.6$  is greater than that in calm water by 13% and 14% respectively. On average, tip circulation in these two conditions is larger than calm water tip circulation whereas it is lower in the case of  $\lambda/L=1.1$ . Interestingly, the trend in the variation of tip circulation is different from the trend seen in cavitation and pressure pulses where the changes in  $\lambda/L=1.1$  and  $1.6$  were much larger as compared to  $\lambda/L=0.6$ .

In order to know if the amount of change in tip circulation can considerably alter the noise level, the possible increase in the inboard noise should be estimated. Noise level at a certain inboard location can be related to the tip vortex index (TVI) as given by [23].

$$dB_{\text{ref}} = 20 \log(TVI \cdot n^2 \cdot D^2) + 20 \log C_1 + 10 \log C_2 \quad (1)$$

$$\text{also, } TVI \propto \Gamma^2 \quad (2)$$

where  $\Gamma$  is blade tip circulation at 12 O'clock position.

Therefore, difference in noise level in the presence of waves as compared to calm water can be written as:

$$dB_{\text{wave}} - dB_{\text{calm}} = 20 \log \left( \frac{\Gamma_{\text{wave}}}{\Gamma_{\text{calm}}} \right)^2 \quad (3)$$

Using Eq. (3) and the results in Figure 32, it is found that the noise level can rise by up to 2 dB due to the change in tip circulation observed in waves.

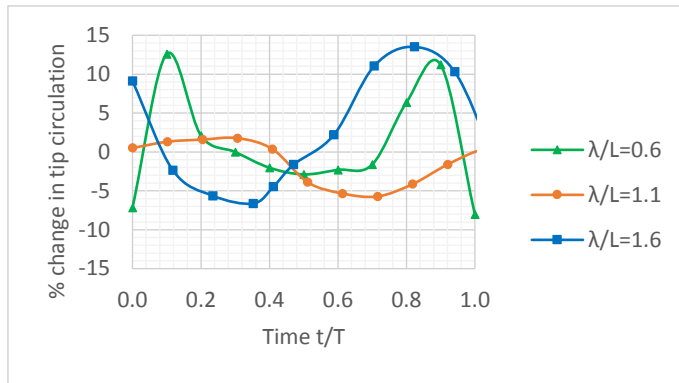


Figure 32 Change in the propeller tip circulation at 12 O'clock position of the propeller blade at different time intervals in waves as compared to the tip circulation in calm water wake.

### 3.2. Effect of increased loading

The ship speed will decrease in the presence of head waves, mainly due to added resistance on the hull. Change in speed will in principle affect the wake variations, both due to changes in motions and in generation of wake in general. Due to the computational expense, the CFD calculations were only performed at the design speed of 14 knots. Therefore, the propeller has been analyzed at 12 and 13 knots in the same set of wake variations observed in the presence of waves at the design speed of the ship, using the same propeller RPM as used in the design speed condition. Speed loss increases the loading on the propeller blades, thus affecting the amount of cavitation. Therefore, increase in the level of pressure pulses due to speed loss in different waves has been studied. The propeller was also analyzed in the calm water wake distribution found for 14 knots at 12 knots speed to compare the rate of change of pressure pulses for different wake distributions as a function of speed loss. The differences in the first harmonic amplitude of pressure pulses obtained at the design speed of 14 knots and reduced speeds of 12 and 13 knots in various wake distributions are presented in Figure 33. The maximum increase in the first harmonic amplitude of pressure pulses due to a speed loss of 2 knots is around 0.58 kPa, and roughly half that value for a speed loss of one knot. Increase in pressure pulses due to speed loss is similar in calm water and waves. Therefore, even if wakes in waves are not available, it is possible to approximate the potential



increase in pressure pulses by calculating the speed loss and using the resulting increase in propeller loading.

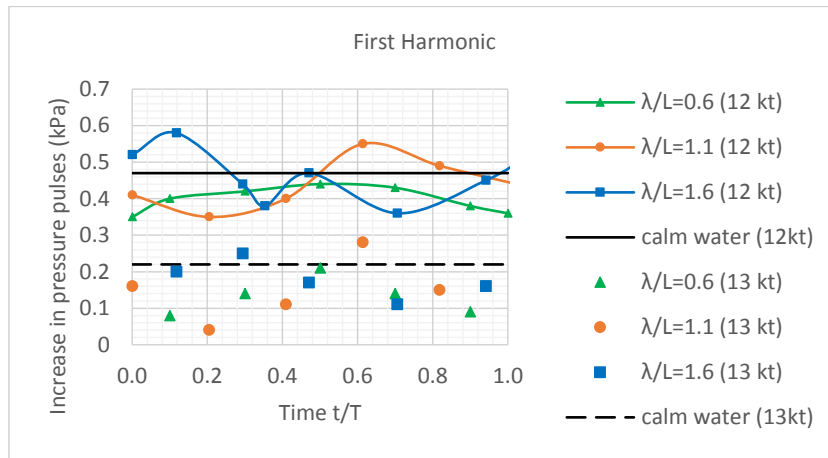


Figure 33 Increase in first harmonic pressure pulses as a result of increased load on the propeller caused by speed loss of 1 and 2 knots, while keeping RPM unchanged.

### 3.3. Effect of RPM fluctuations

The propeller was analyzed at the instant of maximum average wake velocity (meaning minimum Taylor wake fraction) in each wave condition, which corresponds to the instance of maximum RPM. The simulations were performed considering wakes corresponding to those time instances and maximum increase in RPM, estimated based on the method explained earlier. Pressure pulses thus obtained at higher RPM were compared with those obtained in respective wakes at design RPM. Simulations were also performed in calm water wake at highest RPM observed among three wave conditions that is 4.2%. The increase in all three harmonics of pressure pulses in three wave conditions and calm water have been plotted in Figure 34. The increase in first harmonic amplitude is most significant in all four cases, with the maximum increase seen in  $\lambda/L=1.1$  (Note that maximum increase in RPM was observed in this case). The level of increase in first and second harmonic amplitude is comparable in calm water wake and different wave conditions. Therefore, like in the case of increased propeller loading due to speed loss, also the effect

of RPM fluctuation can be estimated by simulating the propeller in calm water wake at higher RPM. Change in third harmonic amplitude is small in all four cases.

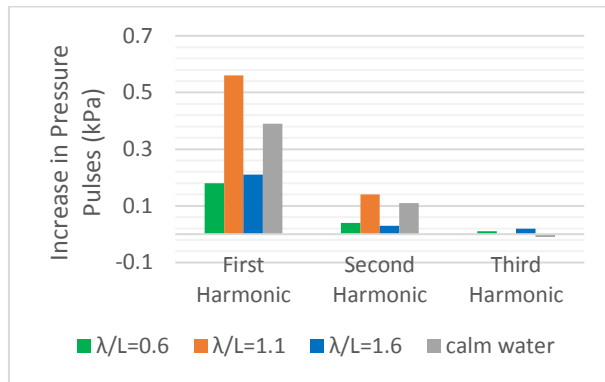


Figure 34 Increase in pressure pulses due to RPM fluctuations in three waves and calm water.

### 3.4. Summary of the factors affecting the pressure pulses in waves

The maximum increase in the first, second and third harmonic of pressure pulses due to different factors is compared in Figure 35. Wake variation has by far the largest influence on all the three harmonics of pressure pulses followed by almost equal influence due to RPM variation and speed loss. The increase in pressure pulses due to wake change is as high as the level of pressure pulses in calm water. The effect of a change in cavitation number due to ship motions and dynamic wave pressure is relatively small on the first harmonic, while the effect is comparable to that due to RPM variation and speed loss on second and third harmonic amplitudes.

RPM variation and ship motions increase the pressure pulses at some time intervals while decreasing at other times, since propeller immersion and RPM oscillates around the mean value. Interestingly, in  $\lambda/L=1.1$  and  $1.6$  where ship motions are considerable, propeller immersion and Taylor wake fraction vary in phase; meaning that the propeller immersion is maximum when Taylor wake fraction is also at its peak. This can be observed by comparing Figure 21 and Figure 26. Consequently, the occurrence of lowest propeller immersion coincides with the highest propeller RPM (because of lowest Taylor wake fraction) both of

which contribute to increase in pressure pulses. In  $\lambda/L=0.6$ , exact opposite is true thus the effect of ship motions on pressure pulses would tend to cancel the effect of RPM fluctuation; however in this case, changes in pressure pulses due to ship motions are small.

From the propeller design point of view, obtaining the wake variation in waves is a challenging task in itself as already mentioned. Therefore, considering the currently available tools, it is difficult to take into account the effect of wake variation in the propeller design. Significant change in the performance was observed both in this case and in the earlier investigations using a single screw ship [11]. Therefore, to limit the required computations while still capturing the main effects of waves in propeller performance, it is recommended to obtain wake variation at least in the critical wave condition (wavelength close to ship length) to have an idea about the possible performance variations due to waves.

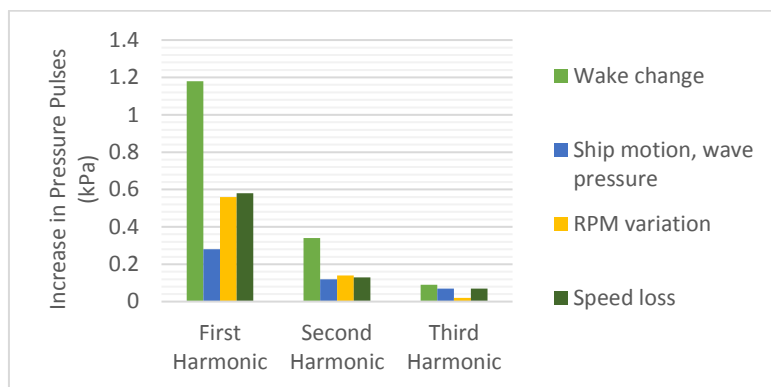


Figure 35 Comparison of maximum increase in pressure pulses due to different factors in the presence of waves.

### 3.5. Efficiency variation in waves

As wake varies substantially in waves, its effect on propeller efficiency should be investigated. Total propeller efficiency in three head waves has been plotted in Figure 36. It can be noted that total propeller efficiency varies significantly in the presence of waves. To investigate the cause of change in efficiency, propeller efficiency, thrust and torque coefficients in calm water and in waves have been plotted in Figure 37 along with propeller open water curves. Since efficiency, thrust and torque coefficients follow open

water curves, it can be concluded that the efficiency is primarily affected by the average change in wake fraction and not much due to variation in nominal wake distribution. Whereas cavitation and pressure pulses are directly related to wake distribution, and they depend less on average wake as discussed earlier.

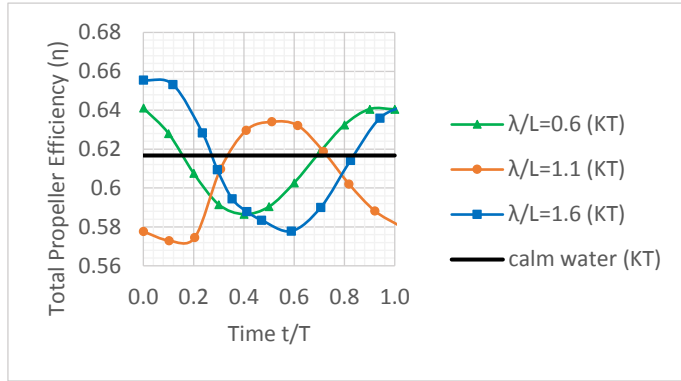


Figure 36 Variation in efficiency in the presence of waves due to wake variation

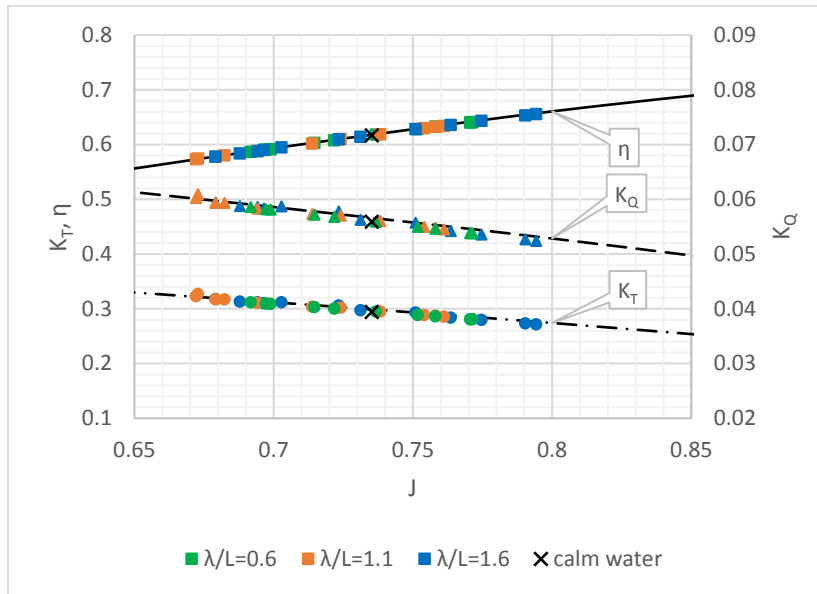


Figure 37 Propeller efficiency,  $K_T$  and  $K_Q$  in the presence of waves along with propeller open water data. Propeller open-water efficiency ( $\eta$ ),  $K_T$  and  $K_Q$  are shown using solid, dash-dot and dashed lines respectively. Efficiency,  $K_T$  and  $K_Q$  in waves are denoted by square, circle and triangle respectively. ( $\lambda/L = 0.6$ –Green;  $\lambda/L = 1.1$ –Orange;  $\lambda/L = 1.6$ –Blue). Cross marks denote the performance in calm water wake.

## 4. Conclusions

Propeller performance of a 8000 dwt chemical tanker with twin Azipull propulsion has been assessed in the presence of waves regarding efficiency, cavitation, and pressure pulses. The effect of wake change,

ship motions, wave dynamic pressure, speed loss, and RPM variation has been considered. It is found that the variation of wake distribution in waves has the largest impact on the propeller performance and the greatest change in cavitation and pressure pulses occurred for waves  $\lambda/L = 1.1$  and  $1.6$ ; changes were relatively small in  $\lambda/L = 0.6$ .

A notable increase in pressure pulses was observed in the analysis of KVLCC2 propeller in the presence of waves [11]. It was believed that the high wake of a full-bodied single-screw ship also lead to strong wake variations due waves. Therefore, it was expected that wake change would be smaller in the case of the current twin-podded case vessel. However, noteworthy wake variations were detected due to waves and ship motions also for the current ship, as shown in section 2.2.

In the analysis reported in [11], wake variation led to higher pressure pulses. However, change in maximum cavitation volume was small. Also, cavity volume variations showed different patterns in the wake in calm water and waves. In the current analysis, both cavity volume and pressure pulses are larger in the presence of waves. However, the pattern of cavity volume variation is similar in calm water and waves for most of the cases. Considering both studies, carried out on different types of hull and propeller designs, propeller performance does differ in the presence of waves. Therefore, analyzing the propeller performance in the presence of waves is recommended when designing the propeller.

While designing the propeller, there is a trade-off between the allowable level of pressure pulses and efficiency. Restricting the level of pressure pulses also limits the maximum efficiency that can be achieved. It is possible that in the absence of any knowledge about pressure pulses in a rough sea, a conservative estimate is applied thus leading to low pressure pulses at the cost of efficiency. Therefore, if pressure pulses in realistic operating conditions can be calculated, the further increase in the efficiency can be achieved while still avoiding detrimental effects due to waves. However, getting wake data for operation

in waves is hard. Thus, we recommend that the wake field in a regular wave of a wavelength close to ship length should be taken into account in the design, in addition to the calm water wake field.

In the view of a substantial increase in the cavitation volumes in the presence of waves, further investigations are necessary to find out if the erosivity of the cavitation is getting affected due to wake change, since even a small amount of erosive cavitation can damage the propeller.

## 5. Acknowledgement

This work is funded by the project 'Low Energy and Emission Design of Ships' (LEEDS, NFR 216432/O70) where the Research Council of Norway is the main sponsor. We are grateful to Rolls-Royce Hydrodynamic Research Centre along with the University Technology centers of Rolls Royce at NTNU and Chalmers University of Technology for their support. We also thank Professor Bjørnar Pettersen from NTNU and Leif Vartdal from Rolls Royce Marine, Norway for insightful discussions and suggestions.

## REFERENCES

- [1] Moor D.I., Murdey D.C. Motions and Propulsion of Single Screw Models in Head Seas, Part II. The Royal Institution of Naval Architects. 1970; Vol 112(2).
- [2] Nakamura S., Naito S. Propulsive performance of a container ship in waves. J. Soc. Naval Archit. Jpn. 1975; Vol 158.
- [3] Guo B.J., Steen S., Deng G.B. Seakeeping prediction of KVLCC2 in head waves with RANS. Applied Ocean Research. 2012; Vol 35: 56-67. <http://dx.doi.org/10.1016/j.apor.2011.12.003>
- [4] Wu P.C. A CFD Study on Added Resistance, Motions and Phase Averaged Wake Fields of Full Form Ship Model in Head Waves [Doctoral Dissertation]: Osaka University; July 2013.
- [5] Albers A.B., Gent W.v. Unsteady wake velocities due to waves and motions measured on a ship model in head waves. 15th Symposium on Naval Hydrodynamics, 1985.

- [6] Hayashi Y. Phase-Averaged 3D PIV Flow Field Measurement for KVLCC2 Model in Waves [M. Sc. Thesis (in Japanese)]: Osaka University; 2012.
- [7] Chevalier Y., Kim Y.H. Propeller Operating in a Seaway. PRADS'95, Seoul, Korea, 1995.
- [8] Jessup S.D., Wang H.-C. Propeller Cavitation Prediction for a Ship in a Seaway. DTIC Document; 1996.
- [9] ABS. Guidance notes on ship vibration. Houston, USA; April 2006 (Updated January 2015).
- [10] VERITEC. Vibration control in ships. Høvik, Norway: A.S. Veritec Marine Technology Consultants, Noise and Vibration Group; 1985.
- [11] Taskar B., Steen S., Bensow R.E., Schröder B. Effect of waves on cavitation and pressure pulses. Applied Ocean Research. 2016; Vol 60: 61-74. <http://dx.doi.org/10.1016/j.apor.2016.08.009>
- [12] He L., Tian Y., Kinnas S.A. MPUF-3A (Version 3.1) User's Manual and Documentation 11-1. Ocean Engineering, University of Texas at Austin; 2011.
- [13] Larsson L., Stern F., Visonneau M., Hino T., Hirata N., Kim J. Proceedings, Tokyo 2015 Workshop on CFD in Ship Hydrodynamics2015.
- [14] Alterskjær S.A. R&D8000 phase I, calm water tests with 3 different fore ships. MARINTEK; 2010.
- [15] Fathi D.E. ShipX Vessel Responses (VERES), User's Manual. MARINTEK; 2016.
- [16] Alterskjær S.A. R&D8000 phase I, head sea tests with 3 different fore ships. MARINTEK; 2011.
- [17] Taskar B., Yum K.K., Steen S., Pedersen E. The effect of waves on engine-propeller dynamics and propulsion performance of ships. Ocean Engineering. 2016; Vol 122: 262-277. <http://dx.doi.org/10.1016/j.oceaneng.2016.06.034>
- [18] Taskar B., Steen S. Analysis of Propulsion Performance of KVLCC2 in Waves. Fourth International Symposium on Marine Propulsors, Austin, Texas, USA, 2015.
- [19] Sun H., Kinnas S.A. HULLFPP, Hull Field Point Potential, User's Manual and Documentation. University of Texas, Austin; 2007.
- [20] Hwang Y., Sun H., kinnas S.A. Prediction of Hull Pressure Fluctuations Induced by Single and Twin Propellers. Propellers/Shafting '06 Symposium, SNAME, Williamsburg, VA. , 2006.

[21] Carlton J.S. Marine propellers and propulsion (Third Edition). Oxford: Butterworth-Heinemann; 2012.

[22] Odabasi A.Y., Fitzsimmons P.A. Alternative Methods for Wake Quality Assessment. International Shipbuilding Progress. 1978; Vol 25: 8 p.

[23] Raestad A.E. Tip vortex index-an engineering approach to propeller noise prediction. The Naval Architect, July/August 1996.